OPEN ACCESS

Saudi Journal of Civil Engineering

Abbreviated Key Title: Saudi J Civ Eng
ISSN 2523-2657 (Print) | ISSN 2523-2231 (Online)
Scholars Middle East Publishers, Dubai, United Arab Emirates
Journal homepage: https://saudijournals.com/journal/sjce/home

Original Research Article

Comparative Study of the Influence of the Fish Coefficient and Young's Modulus with the Hardening Soil Model and The Mohr-Coulomb Model on the Behavior of Cable-Stayed Bridge Piles

Joseph Arsène Bockou Ekockaut[1,2], Louis Ahouet[1,2,3*], Sylvain Ndinga Okina[1,2]

[1]Higher Institute of Architecture, Urbanism, Building and Public Works, Denis Sassou Nguesso University, Congo
[2]Higher National Polytechnic School (ENSP), Marien Ngouabi University – Brazzaville, Congo
[3]Control office for Building and Public Works (BCBTP) – Brazzaville, BP 752, Congo

DOI: https://doi.org/10.36348/sjce.2025.v09i01.001 | **Received:** 05.12.2024 | **Accepted:** 19.01.2025 | **Published:** 22.01.2025

***Corresponding author:** Louis Ahouet
Higher Institute of Architecture, Urbanism, Building and Public Works, Denis Sassou Nguesso University, Congo

Abstract

This article deals with the behavior of isolated piles subjected to two models used in geotechnics (Hardening Soil and Mohr Coulomb) under cyclic lateral loading and their head deformations compared to monotonic loading in sandy soil. The behavior of the cable-stayed bridge piers was predicted using PLAXIS 2D software, based on the results of in situ and laboratory geotechnical studies carried out by the control office for Building and Public Works (BCBTP). Numerical simulation is an alternative to the high cost of large-scale in situ and laboratory studies for describing the behavior of deep foundations. The results obtained show that piles subjected to lateral head loading cause a horizontal head displacement compared with the Hardening Soil and Mohr Coulomb models. Cyclic loading of a pile results in deformation of the soil mass at the surface. Lateral displacement increases with the first few cycles until it stabilizes, generating an irreversible residual displacement due to progressive soil plasticization. Lateral cyclic loading has a favorable influence on pile behavior under cyclic loading, due to the reversible effect on pile displacement.

Keywords: Cyclic Loading, Hardening Soil Model, Mohr Coulomb, Sand, Pile Modeling.

1. INTRODUCTION

Civil engineering structures with piles founded in poor-quality soil layers can absorb all or part of the loads applied to the structure. Significant difficulties then arise in dimensioning methods when these structures are subjected to actions of a repetitive or cyclic nature. Several theoretical, laboratory and full-scale studies on deep foundations subjected to cyclic vertical and lateral loads have been carried out in the past [1-5]. A great deal of work is currently underway to find a solution to the problem of lateral cyclic loading. Structures at sea or on land can be subject to cyclic stresses induced by traffic, waves, wind or other phenomena. This calls for a specific approach to the design of deep bridge foundations. Laboratory studies of pile behavior under cyclic loading have been carried out for many years, using physical and numerical simulations (Boulon *et al*.,) [6]. Variable and repetitive loads are applied over a number of cycles with a constant amplitude and period. These loads can pose problems for pile stability and durability during the operational phase of foundations founded on soils with low bearing capacity. In fact, the soil-pile connection under cyclic loading depends on the type of soil. Indeed, Randolph and Gouvenec (2011) [7], (in their work on clay and sandy soils under stress) note that during cyclic loading applied to a clay, there is an increase or dissipation of pore pressure, a degradation of undrained shear strength and an accumulation of permanent displacements. Sand subjected to cyclic loading is associated with liquefaction potential, displacement accumulation and a possible increase in pore pressure, which depends on the frequency of loading and the permeability of the sand. The modeling also develops graph-based conceptual reasoning for the evaluation of predictive systems involving massive data processing through the integration of artificial intelligence (AI) and a posteriori bridge condition inspection. Given the high cost of large-scale laboratory testing, this study uses numerical simulation as a viable alternative for analyzing problems related to the operation of bridge structure

piers. The Plaxis code offers several types of model for dimensioning civil engineering structures. Our study focuses on the behavior of piles under cyclic lateral loading, with a comparison between the hardening soil model and the Mohr Coulomb model. The aim of this work is to predict the behavior of the cable-stayed bridge's substructure under cyclic loading, in order to assess the soil-infrastructure link and program the monitoring of the structure in its operational phase.

2. MATERIALS AND METHODS

The cable-stayed bridge spanning a depression is located on the corniche of the city of Brazzaville, on the banks of the Congo River. The study is based on geotechnical studies carried out in situ, using pressiometric soundings and intact cores at depths of 10 to 15 m, and tests at the national laboratory of Public Works (BCBTP). The results of investigations at the site identified by drilling show that at a depth of 10 to 15 m, silt-clay sediments are found along the river, topped at the surface by a sandy cover. Beyond a depth of 15 m, the soft sandstone bedrock of Stanley Pool is encountered, with marly or sandy layers, more or less cemented. The physico-mechanical characteristics of the soils on the project site are given in Table 1.

Table 1: Mechanical properties of material layers

Trainning	Depth (m)	PL (MPa)	E_M (MPa)	Internal friction coefficient (Φ)	Cohesion not Drained (C_U)	Wet Density γ_h (KN/m^3)	Dry soil density γ_d (KN/m^3)	Water content W (%)
Silty-clay sediments	0 to 10 (River bank)	0.40	4	-	0	-	-	-
Sands Soft sandstone	10 to 20 > 20m	0.70 5	7 50	28	5	21	18	17

Volumetric weights are determined by soil mechanics formulas. The void index (e) and porosity (n) are determined by the following formulas:

$e = w\,\% \times G_s \Rightarrow e = 0{,}17 \times 2{,}65 = 0{,}45$ (1)

$n = \frac{e}{1+e} \Rightarrow n = \frac{0{,}45}{1+0{,}45} = 0{,}3$ (2)

The shear modulus (Gs) is set at 2.65.

Plaxis 2D is a program designed to analyze the deformations and stability of structures for various geotechnical applications. The program produces a plastic calculation, a consolidation analysis and a variable analysis. It can be used to analyze elastic, elastoplastic and elastoviscoplastic problems in 2D or 3D and in large displacements using the updated Lagrangian method. Table 2 shows sand data from the Batéké series and pile characteristics processed with Plaxis 2D software.

Table 2: Processing of geotechnical soil data and pile mechanical properties using plaxis 2D software version 8.2.

Parameters	Symbol	Values
	Pile property	
Normal stiffness (KN/m)	EA	100995.57e^3 227240e^3
Flexural stiffness (KN/m)	EI	25248e^3 127822.52 e^3
Young's modulus (MPa)	E	32164.195
Density of concrete (KN/m^3)	γ	25 25
Fish coefficient	μ	0.2 0.2
Pile section (2 m^2 – 3 m^2)	A	3.14 7.07
Properties	Plaxix data	HSM model
Reference secant modulus (E_M (4 ; 7 ; 50)	E_{50}^{ref}	32 000
Reference unloading module	E_{ur}^{ref}	96 000
Odometer reference module	E_{oed}^{ref}	18 000
Fish coefficient	μ	0.2 0.2
Coefficient	C_U	0 5
Power	M	0.5

The number of cycles is set at 10, the pile length at 20 m and the diameter at 2 m, with a circular shape, while a comparison is made between the two models inserted in the Plaxis code. The different variations in geotechnical characteristics studied in the HSM model (interface and fish coefficient) are chosen for the study in a sand bed of (50 m^2). The loads used for modeling are : 250 KN, 450 KN, 650 KN, 900 KN. The behavior law used for sand is the Hardening Soil Model (HSM) and Mohr Coulomb for the influence of the Young's modulus obtained from the pressuremeter test and the rheological coefficient. This law has a non-linear hyperbolic

behavior based on the well-known model [8]. The plasticity surface is not fixed, as in perfect Mohr-Coulomb (MC) plasticity models. Work-hardening is allowed in shear and simple compression (isotropic work-hardening). This model was developed for the behavior of powdery soils. The HSM (Hardening Soil Model), implemented in the Plaxis calculation code, is a hyperbolic model originally established by Kondner (1963), then taken up by Duncan and Chang (1970) [9], supplemented by the use of plasticity theory and the introduction of load surface and soil expansion. It comprises 8 parameters (m - an adjustment parameter that depends on soil type ; E50 réf - reference secant Young's modulus, at 50% of deflection at break, under confinement stress $\sigma^3 = P^{réf} = 100$ kPa ; $E_{oed}^{réf}$ - reference odometer module for $\sigma^3 = P^{réf}$; $E_{ur}^{réf}$ - reference unloading module ; υ_{ur} - load-unload Poisson's ratio ; c, ϕ and ψ, $\alpha = 0,5$; E - Young's modulus - Mohr-Coulomb plastic parameters). The different moduli were evaluated at mid-height of each layer and the reference moduli were deduced from the formulas below and the equivalence diameter proposed by the Plaxis finite element calculation :

$$E_{oed}^{ref} = \frac{E_{50}^{ref}}{\frac{E_{50}}{E_{oed}} \times \left(\frac{1}{K_0}\right)^m} \; E_{50} = \frac{2E_M}{\alpha} \; (3)$$

$$K_0 = 1 - \sin\varphi \; E_{oed} = \frac{E_{50}}{1,3} \; (4)$$

$$D_{eq} = \sqrt{\left(\frac{12E_P I_P}{E_P A_P}\right)} \; \upsilon_{ur} = 0,2 \; (5)$$

$$E_{ur}^{ref} = 3 \times E_{50}^{ref} \; E_{50}^{réf} = \frac{4E_M}{0,5} \; (6)$$

$$E = \frac{E_M}{\alpha^2} \; (7)$$

E_M – Module préssiométrique, α^2 – coefficient rhéologique

This study models the behavior of an insulated pile under monotonic and cyclic lateral loading, based on geotechnical and geometric data using Plaxis 2D software.

3. RESULT AND DISCUSSION

3.1 Influence of the Fish Coefficient in the Hardening Soil Model (HSM)

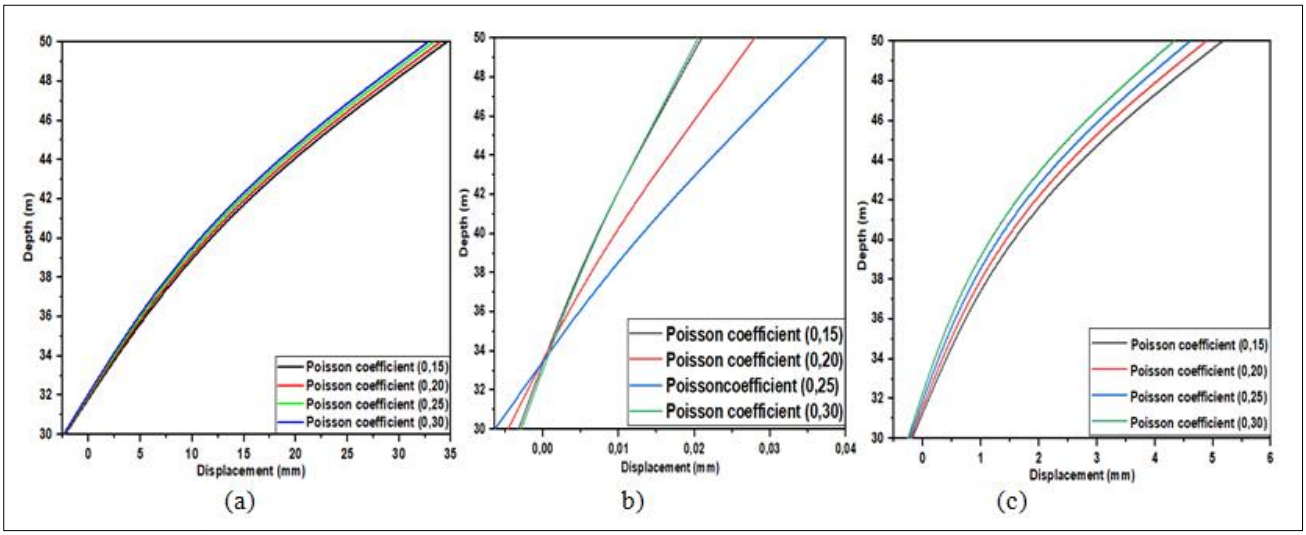

Figure 1(a, b, c): Deformation curve of an insulated pile under monotonic and cyclic lateral loading as a function of the fish coefficient in sand

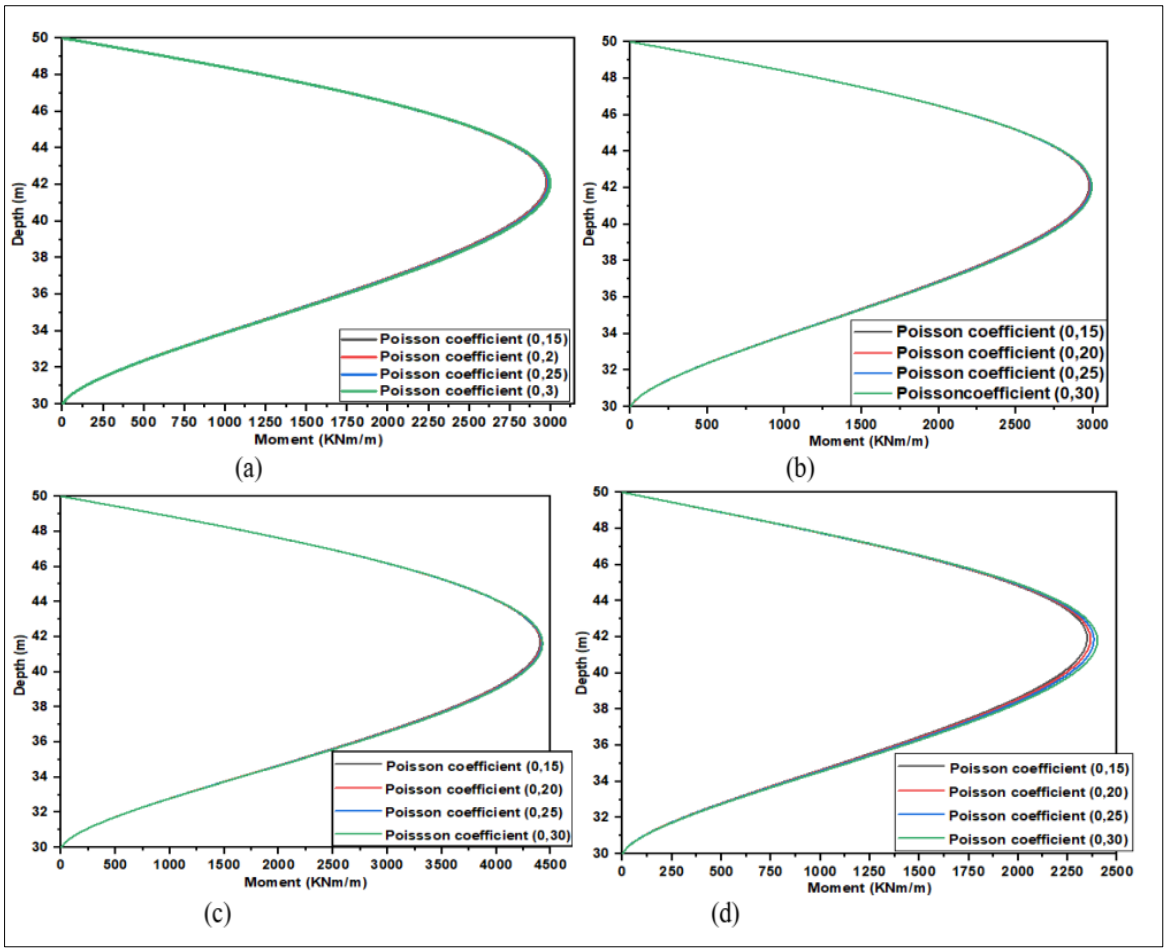

Figure 2 (a, b, c, d) : Different bending moment curves under static and cyclic loading under the influence of the fish coefficient in sand

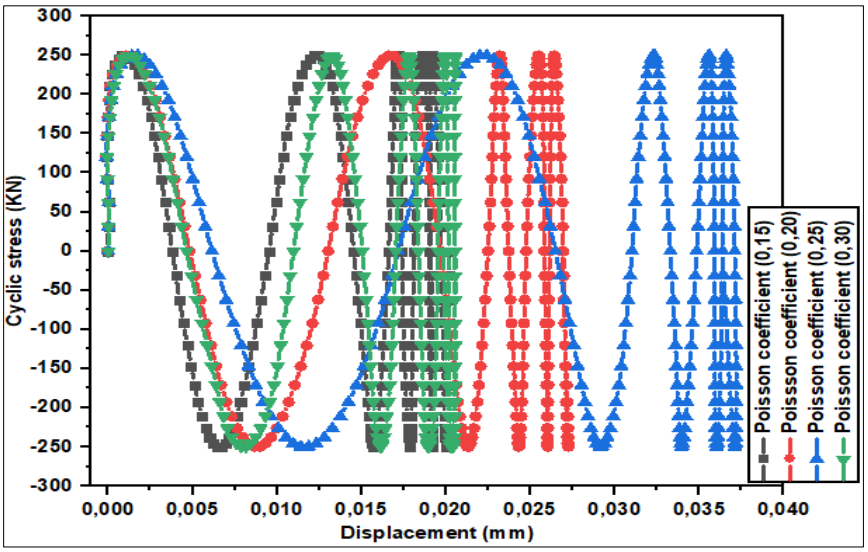

Figure 3 : Cyclic force-displacement curves as a function of the fish coefficient in sand

Figures 1a, 1b and 1c show, through the variation of the fish coefficient, that piles are strongly affected by excessive lateral displacements. This is because the fish coefficient is a factor characterizing the lateral deformability of the soil. Figures 1a and 1c show the lateral displacements under a static load of 650 KN, 450 KN (before and after) and a cyclic load of 250 KN for any value of the fish coefficient (0.15; 0.2; 0.25 and 0.3). The greatest deformations are observed for the smallest value and decrease with coefficient variation, equal to (34.59 mm, 33.96 mm, 33.33 mm and 32.77 mm) and illustrating a 3.50% difference between coefficients (0.15 and 0.3).

Figure 1b shows deformations differing from those obtained under static cyclic loading (before and after). Under monotonic cyclic post-loading, the displacement curves are steeper for higher coefficients. And we observe displacements of the order of (0.02095 mm, 0.0279 mm, 0.0374 mm and 0.0205 mm), with coefficients (0.2 and 0.25) we experienced strong and slight deformation at the pile head under cyclic lateral loading, the difference being 44.11% between coefficients 0.15 and 0.25.

Figures 2a, 2b, 2c and 2d show the evolution of the bending moment under the influence of the fish coefficient. Bending moments vary with increasing fish coefficient under static and cyclic loading, with moments increasing and decreasing with a coefficient value equal to 0.15.

Figure 3 shows the influence of the fish coefficient on the behavior of insulated piles under cyclic stress-displacement. Displacements increase with variation in the fish coefficient. We recorded excessive deformation for the 0.25 coefficient of 0.038 mm compared to the 0.15 coefficient of 0.0202 mm, with a difference of 46.84% between the 0.15 and 0.25 coefficients. The fish coefficient therefore has a negative influence on pile behavior under cyclic loading.

3.2. Influence of Young's modulus in the system Hardening Soil Model (HSM)

Figures 4 (a, b), 5 (a, b) and 6 show the behavior of insulated piles under monotonic cyclic loading (before and after) as a function of Young's modulus [10, 11].

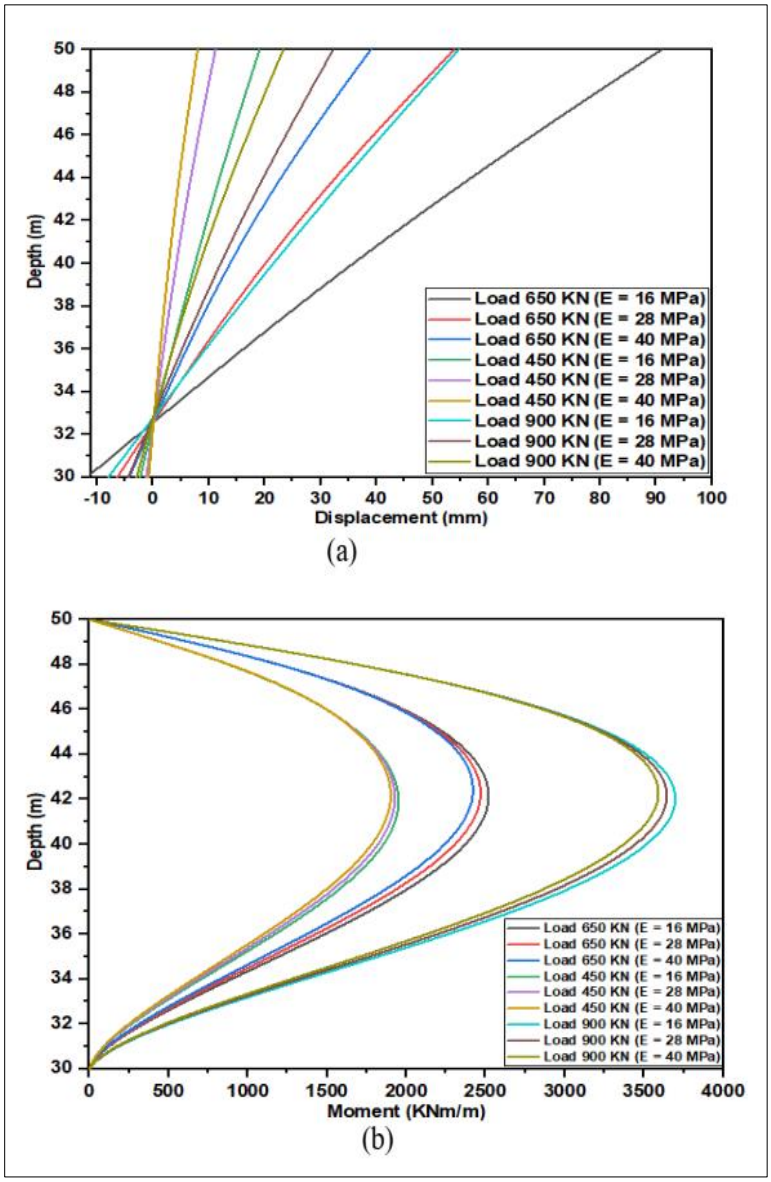

Figure 4 (a, b): Displacement and moment curves of isolated piles subjected to cyclic (before and after) static lateral stress as a function of Young's modulus in Batéké series sand

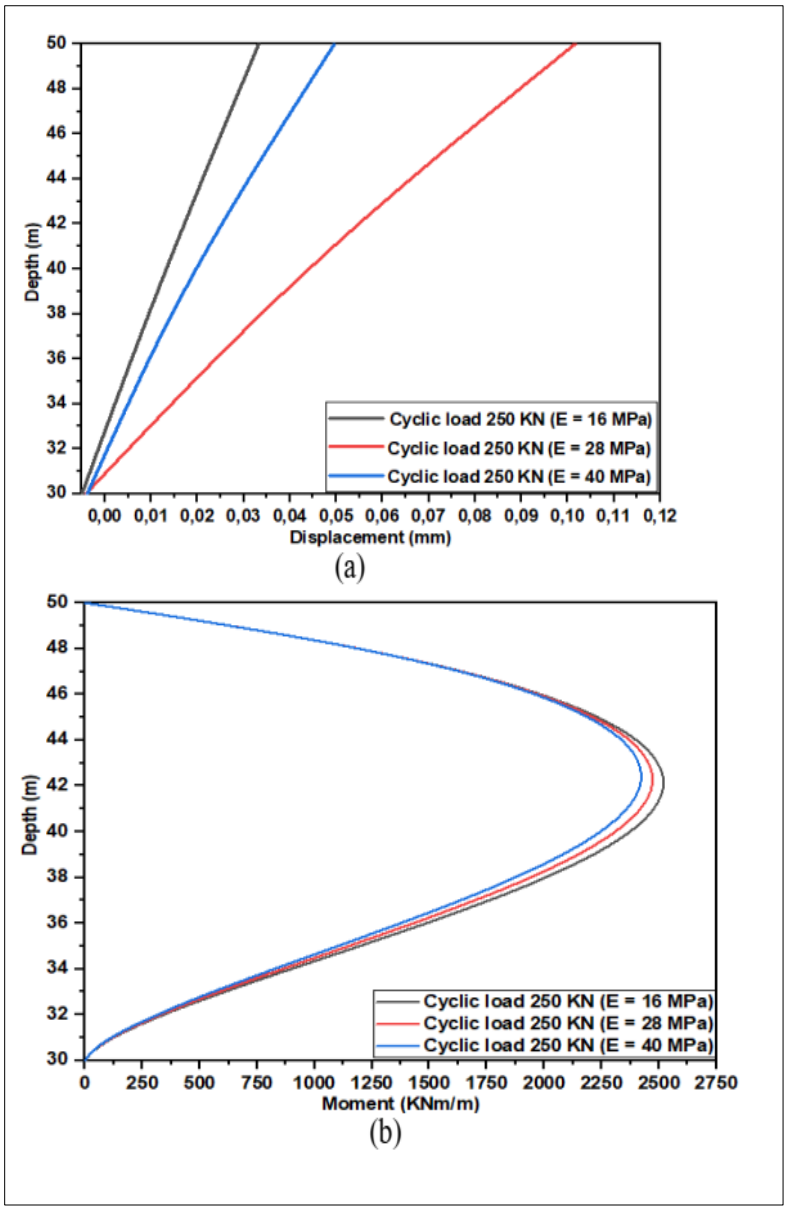

Figure 5 : Representation of displacement and moment curves under cyclic loading as a function of different Young's modulus

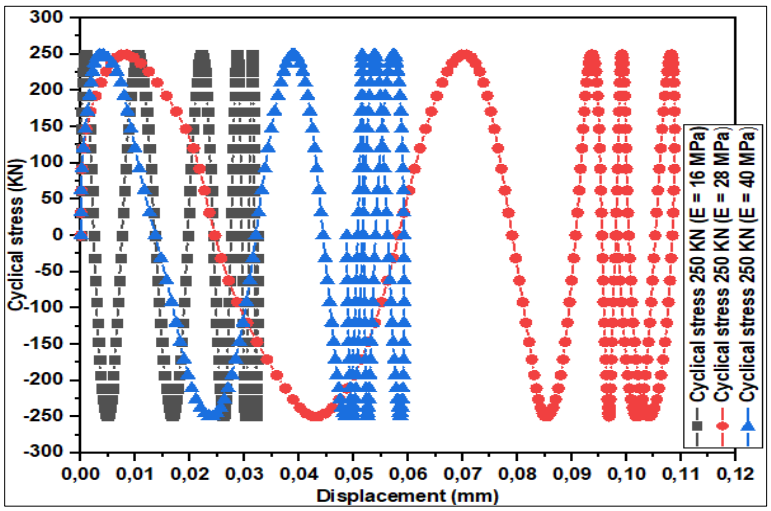

Figure 6 : Evolution of different cyclic stress-displacement curves as a function of Young's modulus

Figure 4a shows the lateral displacement of the pile as a function of different Young's moduli. As the Young's modulus increases under pre-cyclic static loading, a decrease in lateral deformation is observed. The displacements recorded with moduli (16 MPa, 28 MPa, 40 MPa) at a load of 650 KN are of the order of (90.99 mm, 53.88 mm, 38.96 mm). The difference in displacement is of the order of 57.18%, i.e. between (16 MPa - 40 MPa). After cyclic loading, displacement decreases by (19.10 mm, 11.164 mm, 7.97 mm) for a final load of 450 KN. Increasing the final load to 900 KN results in displacements of the order of (54.69 mm, 32.23 mm and 23.31 mm) as a function of cyclic lateral load.

The moment curves shown in Fig. 4b vary with the intensity of the applied load, decreasing with increasing Young's modulus. For moduli of 16 MPa, 28 MPa and 40 MPa respectively, different maximum moment values were recorded: 2518 KNm/m, 2468 KNm/m and 2420 KNm/m respectively, for a static load of 650 KN. The difference in moment is of the order of 3.90%.

Figure 5a shows the evolution of lateral displacement at the pile head under cyclic loading (250 KN) as a function of Young's modulus. Thanks to the rearrangement of soil grains around the pile by cyclic loading, lateral deformation decreases as a function of Young's modulus. For a modulus of 16 MPa, the displacement is of the order of 0.03324 mm, while increasing the modulus to 28 MPa increases the displacement by 0.101 6 mm, and for a modulus of 40 MPa, the displacement decreases by 0.04961 mm. In other words, the 28 MPa modulus appears to be close to its fixing point, beyond which the displacement no longer increases, but decreases. The difference in head displacement is 67.28%.

Figure 5b shows the bending moment curves under cyclic loading as a function of Young's modulus variation. Bending moments remain almost constant compared to post-static moments under a 650 KN load. Increasing the Young's modulus by 16 MPa, 28 MPa and 40 MPa results in moment decreases of the order of 2519 KNm/m, 2471 KNm/m and 2422 KNm/m, i.e. a moment difference of 3.85%. In other words, cyclic loading has little influence on the bending moment developed in the pile.

A close look at Figure 6 shows a decrease in stress-displacement with modulus 16 MPa, a slight increase in stress-displacement with modulus 40 MPa and a significant displacement with modulus 28 MPa. The 28 MPa modulus has an unfavorable influence on pile behavior during cyclic stress-displacement. For the 16 MPa modulus, we recorded a displacement of 0.0323 mm and for the 28 MPa modulus, on the other hand, a slight increase in displacement of 0.1088 mm with the 28 MPa modulus and a decrease of 0.0592 mm with the 40 MPa modulus. The percentage difference between displacement and cyclic stress-displacement is 70.31%.

3.3 Comparison of Hardening Soil Model (HSM) and Mohr Coulomb (MC)

Figures (7a, 7b 8a; 8b and 9) show the different curves for lateral displacement and bending moment of isolated piles under static and cyclic loading according to the models (hardening soil model and Mohr Coulomb).

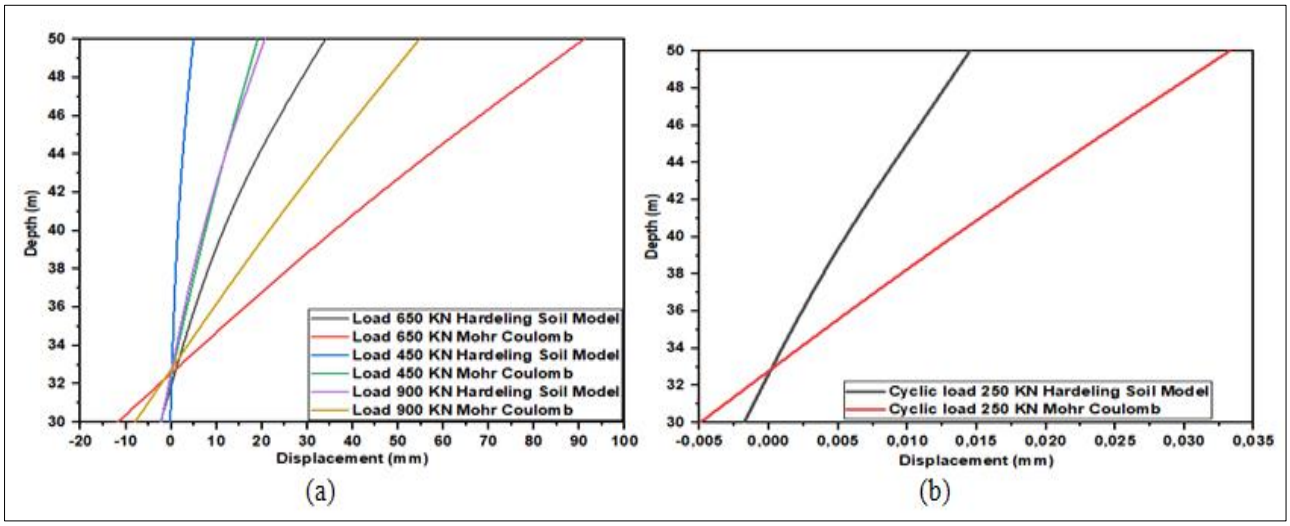

Figure 7: Displacement comparison curve between HSM and MC models under static lateral loading (before and after) and cyclic loading

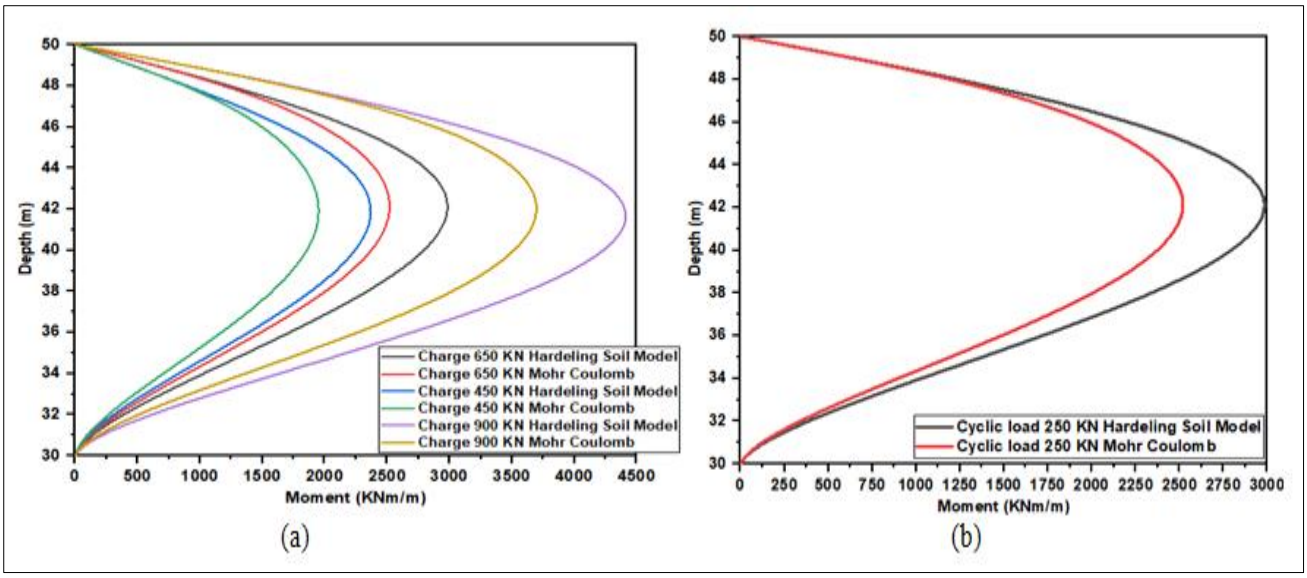

Figure 8: Bending moment comparison curves under the influence of the HSM and MC models under static and cyclic lateral loading in sand

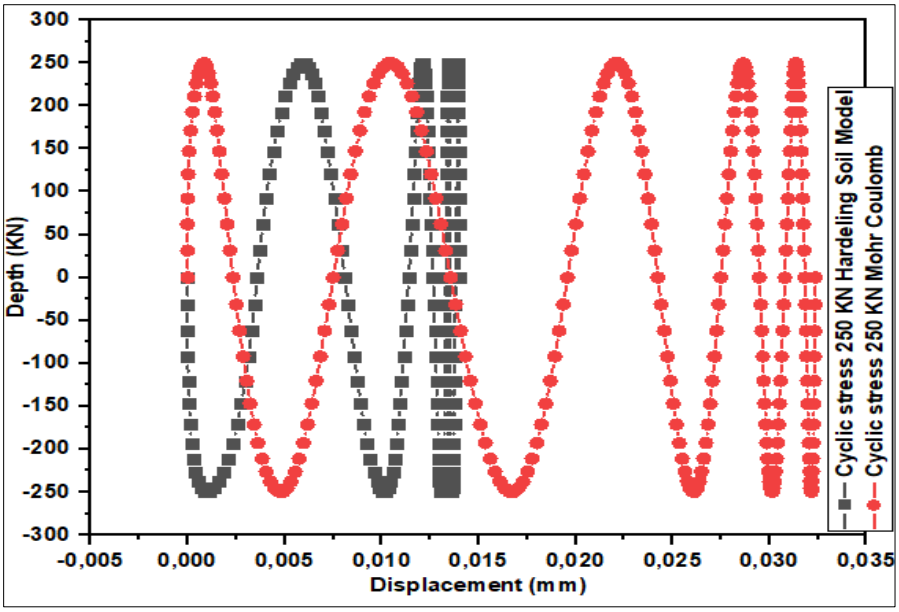

Figure 9: Cyclic stress-displacement comparison curve between HSM and MC models under cyclic loading in sand

Figures 4a, 4b, 5a, 5b and 6 show the behavior of isolated piles in sand under static lateral loading (before and after) and cyclic loading, comparing the HSM and MC models.

Figure 4a shows the evolution of lateral displacements of isolated piles under a monotonic cyclic load of 650 KN (before and after). In this figure, a greater lateral deformation (90.99 mm) is observed with the Mohr Coulomb model than with the hardening soil model, which is (33.96 mm), both before and after the cycle. The difference between the two models is 62.67%, and these displacements decrease with the effect of the last static loading cycles (450 KN and 900 KN) after cyclic loading.

Figure 4b shows the difference in cyclic deformation between the two models. Under cyclic loading, the MC model shows a more pronounced deformation than the HSM model. With a displacement of 0.0332 mm for the MC model and a decrease of 0.0144 mm for the HSM model, the differential deformation is of the order of 56.62%.

Figures 5a and 5b show the bending moment curves observed in both models. The hardening soil model shows maximum moments compared with those obtained with the Mohr Coulomb model, as a function of two loadings (static and cyclic) [12, 13]. However, the moment always varies with the intensity of the load applied to the top. Cyclic loading has little influence on moment evolution.

Figure 6 shows the comparison of cyclic stress-displacement of isolated piles in the two models. Cyclic stress-displacement in the Mohr Coulomb model shows large lateral deformations along the pile, while cyclic results are obtained with the hardening soil model.

4. CONCLUSION

The HSM and MC models describe changes in geotechnical and mechanical characteristics, by modeling the soil-pile couple under cyclic lateral loading. Numerical modelling using Plaxis software has enabled us to discern the behaviour of piles under load with the HSM and MC models, when founded on sand. The results obtained in this study show the importance of cyclic lateral loading, which must be taken into account when dimensioning isolated piles in sandy soil. Cyclic loading plays a key role in stabilizing piles subjected to symmetrical alternating cyclic lateral loading. Modeling enables the structural condition of infrastructure to be assessed in real time, reducing the cost and number of laboratory tests. It also helps to improve design, implementation and maintenance practices.

REFERENCES

1. El Naggar, M. H., Abdel-Meguid, M. A., & Shang, J. Q. (1998). Lateral and cyclic responses of model piles in electrically treated clay. *Proceedings of the Institution of civil engineers-ground improvement*, *2*(4), 179-188.
2. Cavey, J. K., Lambert, D. V., Miller, S. M., & Krhounek, R. C. (2000). Observations of minipile performance under cyclic loading conditions. *Proceedings of the Institution of Civil Engineers-Ground Improvement*, *4*(1), 23-29.
3. Taciroglu, E., Rha, C., & Wallace, J. W. (2006). A robust macroelement model for soil–pile interaction under cyclic loads. *Journal of geotechnical and geoenvironmental engineering*, *132*(10), 1304-1314.
4. Basack, S., & Dey, S. (2012). Influence of relative pile-soil stiffness and load eccentricity on single pile response in sand under lateral cyclic loading. *Geotechnical and Geological Engineering*, *30*, 737-751.
5. Jardine, R. J., & Standing, J. R. (2012). Field axial cyclic loading experiments on piles driven in sand. *Soils and foundations*, *52*(4), 723-736.
6. Boulon, M, Chambón, R, & Darve, F (1977). Incremental rheological law for soils and applications using the finite element method, *French geotechnical journal French geotechnical journal*, *2*(9).
7. Randolph, M. F., Gaudin, C., Gourvenec, S. M., White, D. J., Boylan, N., & Cassidy, M. J. (2011). Recent advances in offshore geotechnics for deep water oil and gas developments. *Ocean Engineering*, *38*(7), 818-834.
8. Johnston, I. W., Lam, T. S. K., & Williams, A. F. (1987). Constant normal stiffness direct shear testing for socketed pile design in weak rock. *Geotechnique*, *37*(1), 83-89.
9. Duncan, J. M., & Chang, C. (2002). Nonlinear analysis of stress and strain in soils. In A History of Progress: Selected U.S. Papers in Geotechnical Engineering.
10. Poulos, H. G., & Davis, E. H. (1980). Pile foundation analysis and design. trid.trb.org
11. Poulos, H. G. (1988). *Marine Geotechnics, Unwin Hyman*, Londres, Royaume-Uni.
12. Rosquoët, F, Thorel, L, Garnier, J. (2013). Piles under lateral load in sand: development of degradation laws to take into account the effect of cycles. 18th ICSMGE, Paris, researchgate.net.
13. Rakotonindriana, M. H. J (2009). Behaviour of piles and groups of piles under cyclic lateral loading (Doctoral thesis, National School of Roads and Bridges, Paris).
14. Rosquoët, F., Thorel, L., Garnier, J. (2009). Pile under cyclic lateral load: measurement uncertainties. geotechnique-journal. Org